

Quantum memory for squeezed light

Jürgen Appel*, Eden Figueroa†, Dmitry Korystov, and A. I. Lvovsky

Institute for Quantum Information Science, University of Calgary, Alberta T2N 1N4, Canada‡

(Dated: October 29, 2018)

We produce a pulse of squeezed vacuum at 795 nm in an optical parametric amplifier and store it in a rubidium vapor cell for 1 μ s using electromagnetically induced transparency. The recovered pulse is analyzed using time-domain homodyne tomography and exhibits up to 0.28 ± 0.05 dB of squeezing. Factors leading to the degradation of squeezing are identified and the phase evolution of the atomic coherence during the storage interval is investigated.

PACS numbers:

Introduction A major challenge in the implementation of quantum communication is the transmission of light over long distances while preserving its quantum state. A proposed solution to this challenge is the implementation of quantum repeaters [1] that enable polynomial, rather than exponential, decrease in the bit transfer rate with distance. The implementation of quantum repeaters requires a quantum memory for optical states.

There exists a variety of approaches to implementing quantum optical memory, for example off-resonant interaction of light with spin polarized atomic ensembles [2] and controlled reversible inhomogeneous broadening [3]. One of the most well-studied techniques is adiabatic transfer between optical quantum states and long-lived atomic superposition using electromagnetically induced transparency (EIT) [4]. This method, proposed in 2000 by Fleischhauer and Lukin [5], has been experimentally demonstrated in 2001 with classical light pulses [6]. In 2005, storage and retrieval of single photons, prepared using the Duan-Lukin-Cirac-Zoller protocol [7], was achieved independently by Chanelière *et al.* [8] and Eisaman *et al.* [9]. These experiments have shown that a quantum state's nonclassical character is preserved after storage and retrieval.

In this letter, we demonstrate compatibility of the quantum repeater technology with the continuous-variable domain of quantum optics by reporting, for the first time, storage and retrieval of the squeezed vacuum state in atomic rubidium vapor. We show that the light in the retrieved mode retains quadrature squeezing, albeit degraded by absorption and atomic decoherence. In addition, we demonstrate that the optical phase of the retrieved squeezed vacuum faithfully reproduces that of the input.

In order to characterize the retrieved state, we use pulsed, time-domain homodyne tomography [10, 11, 12]. This method, allowing complete reconstruction of the quantum state of a specific spatiotemporal mode, has

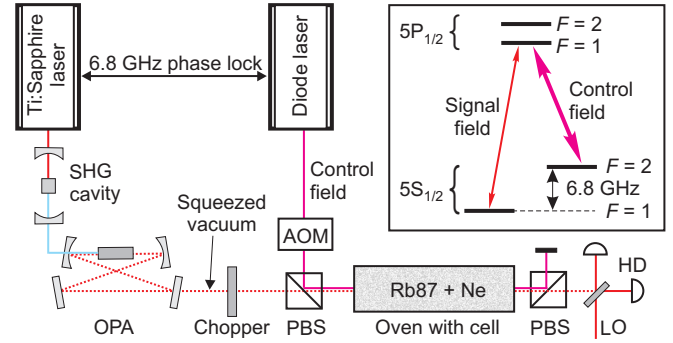


FIG. 1: Experimental setup. The inset shows the atomic level configuration.

been applied to a variety of optical states [13], but not yet to characterization of quantum memories. By using homodyne tomography, we have determined the density matrices of the input and output states, evaluated the memory fidelity and found it to exceed the classical benchmark.

Interaction of squeezed light with atoms under EIT conditions has been investigated by several research groups. Emergence of periodically-poled nonlinear materials enabled construction of narrowband parametric squeezed light sources resonant with atomic rubidium transitions [14, 15, 16]. Propagation and slowdown of squeezed light in an EIT medium has been reported [17, 18, 19] as well as storage of parametric fluorescence [20]. Hsu *et al.* have investigated the effect of propagation through an EIT medium on the quadrature noise of the coherent state and found the atomic gas to generate a large excess noise at low sideband frequencies [21]. This noise has been further studied theoretically and a set of benchmarks for quantum memory performance has been elaborated by Hétet *et al.* [22].

Experimental setup (Fig. 1) The master oscillator, a Coherent MBR-110 Ti:Sapphire laser with a narrow spectral width (~ 40 kHz) and high long-term stability is tuned to the ^{87}Rb $|5S_{1/2}, F=1\rangle - |5S_{1/2}, F=1\rangle$ transition at 795 nm. Its second harmonic, produced by means of a TekhnoScan frequency doubling cavity, pumps our squeezed light source, a degenerate optical parametric

*Present address: Niels Bohr Institute, Blegdamsvej 17 DK - 2100 København, Denmark.

†The first two authors contributed equally to the work.

amplifier (OPA), with a power of 50 mW.

The bowtie cavity of the OPA consists of four mirrors, among which two are flat and two are concave with a curvature radius of 100 mm. The cavity is singly resonant for the generated 795-nm wavelength. We use one of the flat cavity mirrors, with a reflectivity of 93%, as the output coupler. Other cavity mirrors have an over 99.9% reflectivity. The cavity exhibits a 460-MHz free spectral range with a resonant linewidth of approximately 6 MHz. The nonlinear element, a 20-mm-long periodically poled KTiOPO₄ crystal, is placed at the beam waist between the curved mirrors.

The cavity is locked on resonance by means of an additional diode laser phase locked to the master oscillator at an offset of 3 OPA free spectral ranges (1.3 GHz). The cavity lock is implemented using the Pound-Drever-Hall method, with a beam modulated at 20 MHz and counter-propagating the generated non-classical mode. When the signal output of the OPA is measured with a homodyne detector, it exhibits, on average, a 3 dB noise reduction with respect to the shot noise in the squeezed quadrature and 6 dB excess noise in the antisqueezed quadrature in the 500-kHz sideband.

Our goal is to observe storage of squeezed light, so the OPA output has to be chopped into microsecond pulses. Because optical losses degrade squeezing, we avoid using electro- or acousto-optical modulators, and employ an ultra-fast mechanical chopper custom-made from a standard computer hard disk. A 50 μm slit (of cylindrical shape with a diameter of 9 mm) is mounted to the rim of the disk. The disk is then positioned so that when rotating, the slit passes through the OPA output beam focused to a 25 μm size. The disk control is programmed to a rotation frequency of 250 Hz. For most of the rotation period the squeezed vacuum passes through the chopper wheel unobstructed, which allows us to get information about the phase of the squeezed vacuum (see below). When the slit material enters the beam it interrupts the light for about 70 μs , generates a 600 ns (FWHM) squeezed vacuum pulse and blocks the light for another 70 μs . An intensity waveform of a pulse produced by the chopper acting on a classical laser beam is given by the dashed curve in Fig. 2.

The 2.5-mW EIT control field is provided by a separate diode laser phase locked to the master oscillator. The frequency difference between the signal and control fields was set to optimize, on one hand, the classical light storage efficiency, and on the other hand, transmission of squeezed light through the cell under EIT conditions. We found these requirements to be best fulfilled when the frequencies of both fields are red detuned from the center of the Doppler-broadened atomic line by $\Delta_{1\text{-photon}} = 530$ MHz. In addition, the transmission of squeezing is improved when the fields are two-photon detuned from the 6834.683-MHz hyperfine splitting resonance by about $\Delta_{2\text{-photon}} = +0.4$ MHz. This is because

the EIT resonance line is asymmetric, so such detuning permits better accommodation of the entire bandwidth of pulsed squeezed vacuum into the transparency window.

The experiments are performed in atomic ⁸⁷Rb vapor at 65°C, using a Λ energy level configuration formed by one of the hyperfine sublevels of the $5P_{1/2}$ state and two hyperfine sublevels of the $5S_{1/2}$ state (Fig. 1, inset). The rubidium vapor cell used for storage has 5 torr of neon buffer gas and is contained in a magnetically shielded oven. The control and signal fields are orthogonally linearly polarized which allows their combination and separation at the oven entrance and exit. The spatial modes of the control and signal fields are carefully matched to each other.

The beam width of the fields inside the cell is 130 μm . This geometry was chosen as a compromise between two factors. On one hand, a narrower beam increases the flight-through decoherence [23] of the atomic ground levels, which reduces the memory lifetime. On the other hand, decoherence of the atomic dark state leads to Raman scattering of the control field into the signal mode. In quadrature measurements of the control field, this emission manifests itself as low-frequency noise [21] which degrades squeezing in transmission through the EIT cell. This noise appears to increase with the beam width.

The control field is on for most of the 4-ms experimental cycle. It is turned off, by means of an acousto-optical modulator, at time $t = 1.95$ μs (as defined by Fig. 2) when most of the signal pulse has entered the cell, and turned back on after the 1 μs storage period. After an additional 4 μs , when the stored signal has been fully retrieved, the control field is turned off again briefly to obtain a clean sample of the vacuum state noise. The intensity waveform associated with the storage and retrieval of a classical laser pulse is given by the solid curve in Fig. 2.

Upon separation from the control field, the signal is subjected to homodyne detection using a local oscillator (LO) derived from the master oscillator. The LO has constant intensity, but its phase was varied, with a period of 2.5 s, by means of a piezoelectric transducer. The homodyne detector uses two Hamamatsu S3883 photodiodes of 94% quantum efficiency and offers an over 6 MHz bandwidth. The signal from the homodyne detector, corresponding to the quantum quadrature noise of the detected field, is fed to a digital oscilloscope and a spectrum analyzer for simultaneous time- and frequency-domain measurements.

The dot-dashed curve in Fig. 2 shows the pointwise variance of 50,000 oscilloscope traces registering the homodyne detector output during the storage/retrieval procedure. When the control field is off and the signal pulse has terminated (2.4 $\mu\text{s} < t < 2.9$ μs), the signal is in the vacuum state, so the detector outputs shot noise. Prior to the beginning of the signal pulse ($t < 1.4$ μs), and upon completion of the storage procedure ($t > 3.5$ μs), when

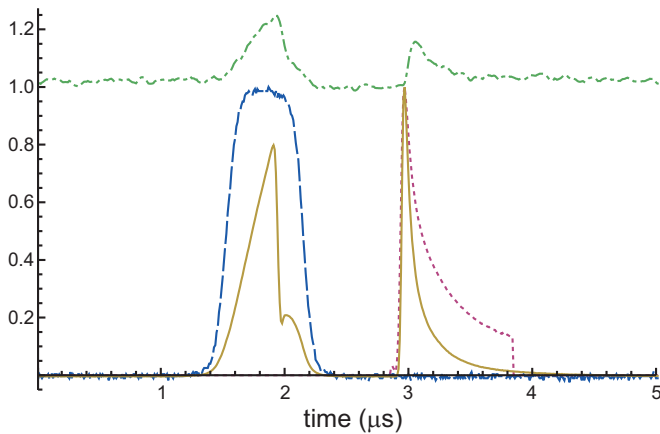


FIG. 2: Time-dependent intensity of the classical input pulse without storage (blue dashed curve), and with storage (yellow solid curve). The y -axis units are arbitrary, but the intensity ratio between the fields is preserved. The green dot-dashed line shows time-domain pointwise variance of quantum quadrature noise as measured by the homodyne detector, normalized to the shot-noise level. The red dotted line is the temporal mode $f(t)$ in which the retrieved state is reconstructed.

the control field is on, the shot noise is elevated by about 0.1 dB due to the Raman scattering mentioned above. When the front of the squeezed vacuum pulse is transmitted through the cell ($1.4 \mu\text{s} < t < 2\mu\text{s}$), the phase-averaged quadrature noise is significantly higher than the shot noise level. When the control field is turned back on after the storage period ($3 \mu\text{s} < t < 3.5\mu\text{s}$), the noise level increases again due to the retrieval of the stored squeezed state.

Quantum state reconstruction We characterize the states of the electromagnetic field modes corresponding to the input and retrieved pulses. We define the temporal amplitude shape $f(t)$ of these modes by the square root of the associated classical intensity waveforms (the mode shape of the retrieved state is shown by the dotted line in Fig. 2). We use a continuous LO, and post-process the homodyne photocurrent by multiplying it by $f(t)$ and subsequently integrating over time [24]. In this fashion, we process the photocurrent from 50,000 retrieved pulses and obtain a set of values that are proportional to the field quadrature noise samples of the retrieved state. The proportionality coefficient is determined from the variance of 50,000 quadrature measurements of the vacuum state acquired in the same temporal mode.

Quantum state reconstruction requires knowing the LO phase values associated with each quadrature sample. This is the purpose of the frequency-domain registration of the homodyne detector output. The spectrum analyzer acquires data continuously in the zero-span mode at a 500 kHz sideband with a resolution bandwidth of 30 kHz and a sweep time of 2.5 seconds. Because this acquisition is relatively slow, and because the chopper

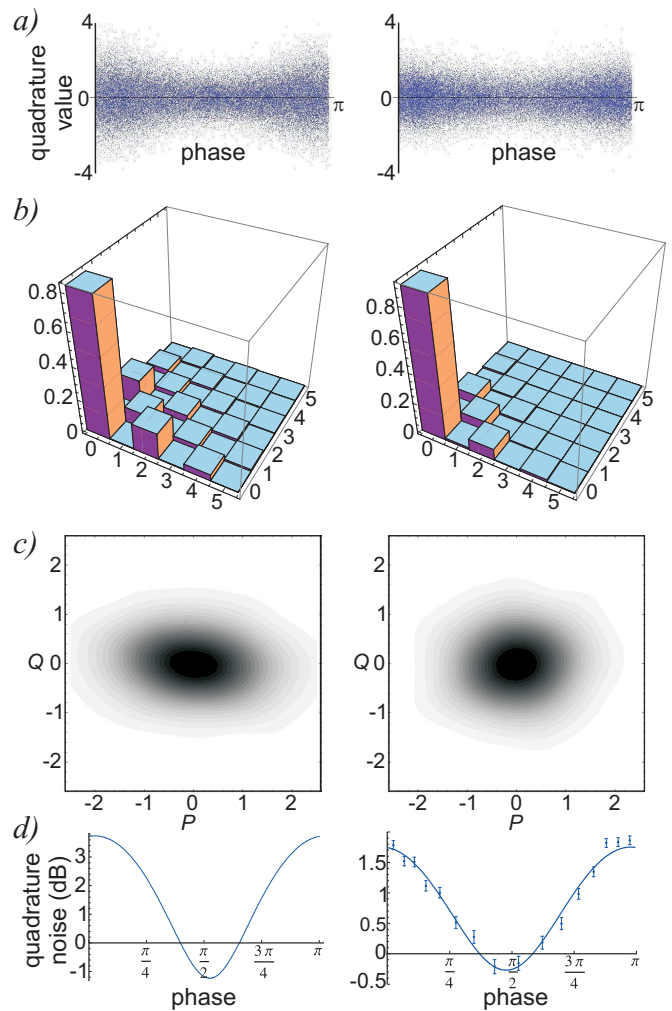


FIG. 3: Quantum state of the input (left column) and retrieved (right column) states. 50,000 samples of phase-dependent quadrature noise (a), maximum-likelihood reconstruction of the density matrices (absolute values, b), Wigner functions (c) and quadrature noise variances (d) are displayed. In (d), the solid lines are calculated from the density matrices while the points with error bars show variances of binned quadrature values, as discussed in the text.

blocks the signal for less than 2% of its rotation period, the chopper has very little effect on the acquired signal, which corresponds to the phase-dependent quadrature noise of the squeezed vacuum generated by the OPA. The LO phase is determined from this signal.

We apply the iterative likelihood-maximization algorithm [25] to reconstruct the input and retrieved states from 50,000 quadrature-phase pairs obtained in this manner [Fig. 3(a)]. This procedure yields the density matrices in the Fock basis [Fig. 3(b)] from which the Wigner function of the state in question is calculated [Fig. 3(c)] as well as the phase-dependent behavior of the quadrature noise [Fig. 3(d)].

Both the input and retrieved states are, to a large ac-

curacy, squeezed thermal states, and both exhibit the minimum quadrature noise at the level below the standard quantum limit. The squeezing for the input state is 1.23 dB and for the retrieved state it is 0.28 dB. The corresponding antisqueezing levels amount to 3.74 and 1.77 dB, respectively. The uncertainty of these values is estimated as described in Ref. [25] as 0.05 dB. We see that the time-domain measurement of the input state already shows significant degradation of squeezing as compared to the frequency domain. This happens because (1) time-domain reconstruction includes low-frequency sidebands, where the squeezing is reduced and additional technical noise is present and (2) in the shoulders of the pulse, the slit edges clip the beam. The squeezing in the retrieved state is further reduced compared to the input. Again, two main factors are at play here. The first one is the storage efficiency, which can be estimated from the classical data to be about 20%. The second degrading factor is the Raman scattering of the control field.

We also verify the presence of squeezing in the retrieved mode by direct calculation of the phase-dependent quadrature variance. To this end, we binned the acquired quadrature values into 16 groups of 3,125 points according to their phases and evaluated the mean square variance of each group [Fig. 3(d), right column]. Two groups exhibit variance below the standard quantum limit, with the difference about twice as high as the margin of error. The latter is evaluated as the statistical error of estimating the width σ of a Gaussian distribution from N samples, and equals $\sigma\sqrt{2/N}$ [26].

We perform two additional tests in order to verify our interpretation of this experiment as demonstration of quantum memory for squeezed light. First, instead of storing the squeezed state, we store vacuum and analyze the quantum state in the retrieved optical mode. As expected, we detect a state with almost phase-independent quadrature noise, elevated by 0.1 dB with respect to the vacuum due to Raman scattering of the control field. Second, we store the squeezed state, but do not turn the control field back on for retrieval. We acquire and analyze the optical state in the same spatiotemporal mode as previously and find, as expected, that, without the control field, this state is almost exactly vacuum.

Fidelity measurement We quantify the performance of our memory setup by means of fidelity, which, for the input and output quantum states $\hat{\rho}_{in}$ and $\hat{\rho}_{retr}$ is defined as $F = \text{Tr}[(\hat{\rho}_{in}^{1/2} \hat{\rho}_{retr} \hat{\rho}_{in}^{1/2})^{1/2}]^2$. Comparing the input and retrieved states, we determine $F = 0.97$. This value is significantly higher than the “classical” fidelity of 0.73, defined by adding two units of the vacuum noise to the input state [27]. The measured fidelity is also higher than 0.82, which would be obtained in a “memory” procedure where the input state is replaced by the vacuum.

Phase evolution We use our setup to study the evolution of the atomic coherence during the storage time with respect to that of the laser fields. If the signal and

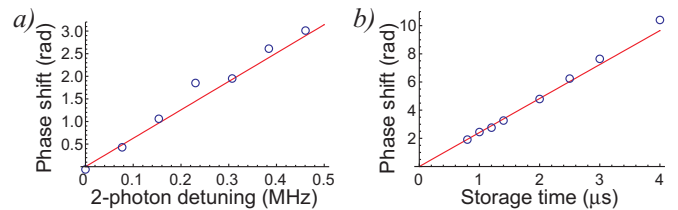


FIG. 4: Phase dependence of the reconstructed squeezed state with respect to the local oscillator as a function of the storage time with a constant $\Delta_{2\text{-photon}} = 384$ kHz (a) and as a function of the two-photon detuning with a constant $\tau_{\text{storage}} = 1$ μs (b). The solid lines correspond to Eq. (1)

control field are not in exact two-photon resonance with respect to the atomic hyperfine splitting, the atomic and optical systems evolve with different frequencies. As a result, the retrieved state’s phase, measured with respect to the local oscillator, is different from the input by

$$\phi = 2\pi\Delta_{2\text{-photon}}\tau_{\text{storage}}, \quad (1)$$

so we expect a linear behavior if either the two-photon detuning or the storage time are changed. We verify this dependence, reconstructing the retrieved state at different values of these parameters. This reconstruction yields phase values modulo π , so in order to fit the theoretical prediction (1) we add multiples of π to each point. The result of this procedure is shown in Fig. 4 and exhibits good agreement with the theory.

Conclusions We have demonstrated storage and retrieval of pulses of squeezed light using EIT. For the first time, complete tomographic characterization of the quantum state after the storage procedure has been performed, exhibiting nonclassical features of the retrieved state in a distinct spatiotemporal mode. We have identified the factors leading to the degradation of squeezing and investigated the phase evolution of the atomic coherence during the storage interval.

Acknowledgements We gratefully acknowledge M. Eisaman, P. Kulchin, F. Vewinger, K.-P. Marzlin and B. C. Sanders for fruitful discussions, as well as G. Günter, Y. Takeno and M. Lobino for their help in the laboratory. This work was supported by NSERC, CIAR, iCORE, AIF, CFI and Quantum Works.

While this paper was being prepared for publication, we became aware of the work [28], where storage and retrieval of squeezed vacuum in a cold atom ensemble has been demonstrated, albeit without tomographic reconstruction.

‡ URL: <http://www.iqis.org/>

[1] H. J. Briegel *et al.*, Phys. Rev. Lett. **81**, 5932 (1998).
[2] B. Julsgaard *et al.*, Nature **432**, 482 (2004).

- [3] B. Kraus *et al.*, Phys. Rev. A **73**, 020302 (2006); S. A. Moiseev and S. Kröll, Phys. Rev. Lett. **87**, 173601 (2001)
- [4] M. Fleischhauer, A. Imamoglu, and J. P. Marangos, Rev. Mod. Phys. **77**, 633, 2005.
- [5] M. Fleischhauer and M. D. Lukin, Phys. Rev. Lett. **84**, 5094 (2000)
- [6] D. F. Phillips *et al.*, Phys. Rev. Lett. **86**, 783 (2001).
- [7] L. M. Duan *et al.*, Nature **414**, 413 (2001).
- [8] T. Chanelière *et al.*, Nature **438**, 833 (2006).
- [9] M. D. Eisaman *et al.*, Nature **438**, 837 (2006).
- [10] D. T. Smithey, M. Beck, M. G. Raymer, and A. Faridani, Phys. Rev. Lett. **70**, 1244 (1993).
- [11] U. Leonhardt, *Measuring the quantum state of light*, Cambridge University Press, 1997.
- [12] A. I. Lvovsky and M. G. Raymer, quant-ph/0511044.
- [13] A. I. Lvovsky *et al.*, Phys. Rev. Lett. **87**, 050402 (2001); A. I. Lvovsky, S. A. Babichev, Phys. Rev. A **66**, 011801 (2002); A. Zavatta, S. Viciani, and M. Bellini, Science **306**, 660 (2004); A. Ourjoumtsev, R. Tualle-Brouri, J. Laurat, P. Grangier, Science **312**, 83 (2006).
- [14] T. Tanimura *et al.*, Opt. Lett. **31**, 2344 (2006).
- [15] G. Hetet *et al.*, J. Phys. B: At. Mol. Opt. Phys. **40**, 221 (2007).
- [16] J. Appel *et al.*, Phys. Rev. A **75**, 035802 (2007).
- [17] D. Akamatsu *et al.*, Phys. Rev. Lett. **92**, 203602 (2004).
- [18] M. Arikawa *et al.*, arXiv:0707.1971
- [19] D. Akamatsu *et al.*, quant-ph/0611097
- [20] K. Akiba *et al.*, quant-ph/0701073
- [21] M. T. L. Hsu *et al.*, Phys. Rev. Lett. **97**, 183601 (2006)
- [22] G. Hétet *et al.*, arXiv:0707.1178
- [23] E. Figueroa *et al.*, Opt. Lett. **31**, 2625 (2006)
- [24] J. S. Neergard-Nielsen *et al.*, Phys. Rev. Lett. **97**, 083604 (2006); J. S. Neergard-Nielsen *et al.*, arXiv:0704:1864.
- [25] A. I. Lvovsky, J. Opt. B: Quantum and Semiclassical Optics **6** S556 (2004); J. Řeháček, Z. Hradil, E. Knill, and A. I. Lvovsky, Phys. Rev. A **75**, 042108 (2007).
- [26] Y. Bar-Shalom and X.-R. Li, *Estimation with Applications to Tracking and Navigation*, John Wiley & Sons, New York, 2001
- [27] P. van Loock, S. L. Braunstein, and H. J. Kimble, Phys. Rev. A **62**, 022309 (2000).
- [28] K. Honda *et al.*, arXiv:0709.1785